

## Brief communication: CMIP6 does not suggest any atmospheric blocking increase in summer over Greenland by 2100

Alison Delhasse<sup>1</sup> | Edward Hanna<sup>2</sup> | Christoph Kittel<sup>1</sup> | Xavier Fettweis<sup>1</sup>

<sup>1</sup> Laboratory of Climatology, Department of Geography, SPHERES research unit, University of Liège, Liège, Belgium

<sup>2</sup> School of Geography and Lincoln Centre for Water and Planetary Health, University of Lincoln, Lincoln, UK

Correspondence

Email: [alison.delhasse@uliege.be](mailto:alison.delhasse@uliege.be)

Funding information

Fonds de la Recherche Scientifique de Belgique, Grant/AwardNumber: 2.5020.11

### ABSTRACT

The Greenland blocking index (GBI), an indicator of the synoptic-scale circulation over Greenland, has been anomalously positive during most summers since the late 1990s. Such changes in atmospheric circulation, favouring anticyclonic conditions, have led to an increase in Greenland summer temperatures, a decrease in cloud cover and larger surface melt. The GBI is therefore a key indicator of melting and surface mass balance variability over the Greenland ice sheet. However, the models of fifth phase of the Coupled Model Intercomparison Project (CMIP5) do not represent the increase in GBI that is suggested by recent observations, and do not project any significant increase in GBI until 2100. In this study the new generation of CMIP6 Earth-system models is evaluated in order to analyze the evolution of the future GBI. All CMIP5 and CMIP6 projections reveal the same trend towards a decrease of the GBI until 2100 and no model reproduces the strong increase in the persistence of summer blocking events observed over the last few decades. Significant melting events related to a highly positive GBI, as observed in summer 2019, are still not considered by CMIP6 models and therefore the projected surface melt increase of the ice sheet could be underestimated if such summer circulation changes persist in the next decades.

### KEYWORDS

Greenland, GBI, Climate, Projections, CMIP6

## 1 | INTRODUCTION

A Greenland Ice Sheet (GrIS) extreme melting event occurred in summer 2019 (Tedesco and Fettweis, 2020) and followed several other exceptional years since the beginning of recordings (eg., 2003, 2005, 2007, 2008, 2010, 2012 and 2015, Fettweis et al., 2013a; Tedesco et al., 2013, 2016; Hanna et al., 2014). The 2019 melt season resulted from specific anticyclonic conditions, especially northwards advection of warm and moist air along the western part of the ice sheet and enhanced absorption of solar radiation strengthening melt, amplified by the melt-albedo feedback (Tedesco and Fettweis, 2020). Although this near-record Greenland melt is due to the combination of anticyclonic conditions with low winter accumulation, it is also part of a series of Arctic summers characterized by blocking events which have become increasingly frequent over the past 20 summers (Fettweis et al., 2013a; Hanna et al., 2014; Belleflamme et al., 2015; McLeod and Mote, 2016). This succession of blocking events over several summers is one of the causes of the negative SMB record of 2012. This record was due not only to the heritage of the snowpack, but also to the

This article has been accepted for publication and undergone full peer review but has not been through the copyediting, typesetting, pagination and proofreading process which may lead to differences between this version and the [Version of Record](#). Please cite this article as doi: [10.1002/joc.6977](https://doi.org/10.1002/joc.6977)

particular atmospheric conditions of a blocking event combined to the increase in surface temperature, exposing bare ice and triggering the melt-albedo feedback (Tedesco et al., 2013).

Blocking events are mainly associated with persistent synoptic-scale ridges of high pressure over Greenland. This means anticyclonic conditions over the ice sheet with more shortwave radiation incoming during summer, reduction in cloud cover (Hofer et al., 2017) and warm air advection from the south-west, which increases surface ice melt due to higher temperatures and the melt-albedo positive feedback.

These more frequent blocking events are one of the main contributors to the recently observed acceleration in GrIS surface melt (Fettweis et al., 2013b; Overland et al., 2012), and have led to a significant decline in the GrIS surface mass balance (SMB) since the 1990s (van den Broeke et al., 2016; Fettweis et al., 2017; Trusel et al., 2018; Noël et al., 2019).

Despite the importance of such dynamical atmospheric changes, they are not represented by any of the CMIP5 Earth-system models (regardless of their complexity level, general models are called ESMs hereafter) for present-day climate (Fettweis et al., 2013b; Hanna et al., 2018a). None of the models suggest any increase in Greenland blocking events by 2100, while some models even suggest moderate decreases in blocking. This model-observation disparity means that the melt increase over the Greenland ice sheet could be underestimated by a factor of two if such changes continue to occur, which might result in ESMs potentially underestimating the future decrease in SMB (Delhasse et al., 2018).

The latest Climate Model Intercomparison Project (CMIP6) provides new projections simulated by an improved generation of ESMs. The most important enhancements compared to CMIP5 are a higher resolution, a more sophisticated physics scheme that most notably includes the improvement of the coupling between the different components of the Earth-system, and better constrained concentrations of aerosols and other near-term climate forcings (Eyring et al., 2016; O'Neill et al., 2016; Voldoire et al., 2019). While the CMIP6 models are forced by similar atmospheric greenhouse gas scenarios, they are more sensitive than CMIP5 due to notably stronger cloud feedbacks (Andrews et al., 2019; Gettelman et al., 2019; Voldoire et al., 2019). For the Greenland ice sheet, a new investigation suggests a doubling of surface melt in CMIP6 models relative to CMIP5 (Hofer et al., 2020).

Considering the impact of such blocking events on the recent increase in Greenland melt, together with the availability of new CMIP6 ESM projections, the aims of this study are to assess: 1) the ability of these new simulations to represent the recent increase in Greenland blocking over the present, and 2) whether such a change in blocking is predicted from now until 2100, bearing in mind that CMIP5 suggests a decrease in summer blocking events over Greenland during the next decades.

## 2 | DATA AND METHODOLOGY

Greenland blocking events are evaluated using the 500 hPa geopotential height (Z500) averaged and area-weighted over the region 60-80 °N, 20-80 °W, defined as the Greenland Blocking Index (GBI, Fang, 2004; Hanna et al., 2013, 2014, 2015, 2016, 2018a, 2020) which is used here to assess the representation in CMIP5 and CMIP6 models of the recent summer blocking events observed over Greenland. The GBI and thus summer Z500 increase reported over these last few decades, is variously and indeterminately influenced by two factors: 1) global climate warming and, 2) atmospheric dynamical changes linked to a more meridional configuration of the polar jet stream that favours anticyclonic conditions over Greenland (Overland et al., 2012). In order to avoid the influence of the global temperature increase (Figure 1) on GBI and to study only the dynamic (and

not thermal) atmospheric changes that (are projected to) occur over Greenland (GR), the GB2 index (Eq. 1, Hanna et al., 2018a) is used here. GB2 is calculated as the normalized difference between GBI and the area-weighted mean Z500 over the northern hemisphere region of 60-80 °N (NH).

$$(1) \quad \begin{aligned} GBI &= Z500_{GR} \\ GB2 &= Z500_{GR} - Z500_{NH} \end{aligned}$$

We also use the free-atmosphere temperature within the GBI region (TA hereafter), defined as the summer mean temperature at 850, 700 and 500 hPa over the GR area (Eq. 2). TA and GBI are closely related (Table 1 and Figure 1).

$$(2) \quad TA = (T_{850} + T_{700} + T_{500})_{GR}$$

GBI, GB2 and TA are based on summer (JJA) CMIP5 and CMIP6 simulations (1950 – 2100) and are compared with the same parameters based on NCEP/NCARv1 reanalysis (Kalnay et al., 1996, NCEP hereinafter) and ERA5 reanalysis (Hersbach et al., 2020) for the following recent period: 1950 – 2019 (1979 – 2019 for ERA5). Only CMIP6 models with outputs available for the high emission scenario (ssp585) (Gidden et al., 2019) are considered in this study (33, listed in Table S2 in supplementary materials). The CMIP5 models used in Hanna et al. (2018a) (considering the RCP8.5 scenario only) are also included and these 35 models are listed in Table S2. The new CMIP6 scenario, ssp585, is approximately equivalent to RCP8.5 in terms of radiative forcing (+8.5 W/m<sup>2</sup>, Taylor et al., 2012; Eyring et al., 2016; O'Neill et al., 2016). For comparison, the NCEP and ERA5 reanalyses are used as references for the recent observed climate (respectively 1948 – 2019 and 1979 – 2019). All time series are presented here in normalized form with respect to the reference period 1980 – 1999. A weighted running mean is applied by using a midpoint-centred 21-year running mean, which shortens the beginning and the end of series by 10 years, as shown in Figure 2.

In addition to the GBI and GB2 based analysis performed by Hanna et al. (2018a) for CMIP5, we will discuss the Z500 projected pattern changes over the 50-90 °N area. Similar to GB2, we define ZG2 for each grid cell as the difference between Z500 of the grid cell and the average Z500 over the 60-80 °N area in order to isolate the Z500 dynamic anomaly from the thermal anomaly. The anomaly of ZG2 with respect to the reference period (1980 – 1999) is calculated as an average for different selected periods.

### 3 | RESULTS

The GBI in the ESMs (from both CMIP5 and CMIP6) increases linearly with the atmospheric (mid-troposphere) temperature (Figure 1), but this increase is smaller than the observed GBI increase. This indicates a shift towards more favourable atmospheric dynamic (jet stream) precursors, in addition to higher temperatures, causing Greenland blocking events. Figure 1 also reveals a stronger CMIP6 warming rate than in CMIP5 for an identical GBI vs TA relationship. On average, CMIP6 models warm by 1 °C compared to CMIP5 models over the period 2081 – 2100. These warming are significantly different (t test,  $\alpha = 5\%$ ). The extreme values of free atmosphere temperatures of CMIP6 models are also shifted by +1 °C with respect to CMIP5 (supplementary materials, Figure S7).

In order to ascertain whether global warming is the main driver of the projected GBI changes, the determination ( $r^2$ ) between GBI and free atmosphere temperature has been calculated for each model over three different periods (1950 – 2019, 2020 – 2100 and 1950 – 2100, Table 1). For the recent period, as for NCEP and ERA5, ESMs-based GBI is not fully dependent on the temperature

( $r^2$  average of 0.51 for CMIP5 and 0.61 for CMIP6). But in the future, the increase in free atmosphere (mid-troposphere) temperature determines the increase in GBI ( $r^2$  average of 0.81 for CMIP5 and 0.87 for CMIP6). Because Greenland climate is expected to continue to warm, leading to an increase in GBI, this justifies the use of GB2 for evaluating future changes in GBI that are not caused by temperature variability.

The NCEP and ERA5 reanalyses show a significant increase in GB2 (larger than the interannual variability where the latter is measured using the standard deviation) over the recent period, which is not represented by any of the CMIP5 and CMIP6 models (Figure 2). In CMIP5, the highest GB2 value does not even reach one standard deviation (std). Between 2000 and 2020 one CMIP6 models (MRI ESM2-0), out of 33, almost reach one std of GB2 and oscillate until the end of the century with a decreasing trend. Around 2040, two other CMIP6 models (EC-Earth3-Veg and NESM3) oscillate near one std and a further one (NorESM2-LM) between 2040 and 2060. Nevertheless almost all the ESMs project a significant ( $p < 0.05$ ) decrease in GB2 by the year 2100 with no projection showing an overall increase in blocking. It should be noted that 3 models do not show a significant trend (2 CMIP5 models: GISS-E2-H, GISS-E2-R, and 1 CMIP6 model: EC-Earth-3).

Table S1 (in supplementary materials) summarizes occurrences of summers characterized by  $GB2 > (<) 1$  (-1) and 2 (-2) for NCEP and ERA5 over the current period, CMIP5 and CMIP6 models (2000 – 2019, 2040 – 2060 and 2080 – 2100). Between 2000 and 2019, the NCEP summer GB2 has been negative six times but only two of these instances occurred since 2007. Out of 2007 to 2019 summers, only 2013, 2017 and 2018 had  $GB2 < 1$  (-2.37, 0.22 and -2.07 respectively, Figure S1 in supplementary materials), highlighting the prevalence of high GB2 values ( $GB2 > 1$ ) during recent summers. For CMIP5 models, the maximum number of occurrences of  $GB2 > 1$  over 2000 – 2019 is 4 for the HadGEM2-CC and ACCESS1-3 models, and only few models (9 out of 35) have summers with  $GB2 > 2$ . In comparison, CMIP6 models seem to show higher summer occurrences of  $GB2 > 1$  over 2000 – 2019 relative to CMIP5; however, the maximum occurrence (8 for MRI-ESM2-0 and NESM3), does not reach the NCEP and ERA5 based observed occurrence (respectively 11 and 10). Up to the end of the century using CMIP6 projections, there is a decrease in the occurrence of positive GB2, which confirms previous finding based on CMIP5 (Hanna et al., 2018a).

Finally, it is important to note that the results presented in this study are insensitive to changing both the chosen reference period (supplementary material Figure S5 and S6) and the length of the running mean (supplementary materials Figure S2 to S4).

Comparing the ZG2 pattern of the ESMs when they suggest high positive GB2 values to the ZG2 pattern of the reanalysis leads to the conclusion that none of the ESMs tested here are able to represent positive anomalies (high pressure) over Greenland of the same magnitude as those observed in NCEP-NCARv1 and ERA5 reanalyses (Figure 3 a and d). Only MRI-ESM2-0 (Figure 3 b), showing a small increase in GB2 for the recent (2000 – 2019) period (Figure 2), has ZG2 anomalies over the current period that correspond to the reanalyses-based one observed over 2000 – 2019; however, this anomaly is insignificant compared to the interannual variability (not shown). One further CMIP6 model, NESM3, simulates a GB2 increase over 2030 – 2050 (Figure 2) but once again, while it has a similar ZG2 pattern (Figure 3 e) to reanalyses for 2000 – 2019, the anomalies are shifted slightly westward and are also insignificant. No other CMIP model shows a similar ZG2 pattern to reanalyses over this century, while CMIP anomalies are generally slightly negative relative to the reference period (for instance Figure 3 c and f) confirming the decrease of GB2 projected by the end of this century.

#### 4 | CONCLUSIONS



Blocking events have more often characterized summers in Greenland since the late 1990s, leading to several ice-melt records including, most recently, in 2019. This reflects generally more blocked atmospheric circulation over Greenland, as gauged by using the GBI index. The GBI has strongly increased since the late 1990s while the previous generation of ESM models (CMIP5) does not reproduce such an increase (Hanna et al., 2018a). In this study we used GB2 to evaluate the ability of the new CMIP6 models to represent the recent variability of the atmospheric circulation over Greenland in summer, as well as its future evolution to 2100. We conclude that no increase in the frequency of Greenland blocking events are revealed for either recent or future climates (1990s to 2100) by the CMIP6 models, and that the free-atmosphere temperature variability fully drives the GB2 changes in the ESM-based projections. This suggests that, according to both CMIP5 and CMIP6 models, recent circulation anomalies could be due to the natural variability. Conversely, as described by Smith et al. (2020), ESMs could indeed simulate a variability of the atmospheric circulation, but too weak and explaining why (future) blocking events in ESMs are minor compared to the observed blocking events.

As shown in Delhasse et al. (2018), atmospheric warming combined with recently observed circulation changes could result in a doubling of the surface melt increase of the Greenland ice sheet. By not resolving a possible sustained increase in future Greenland blocking events and associated atmospheric circulation changes, CMIP6 (and previous CMIP5) ESM-based projections could therefore underestimate Greenland ice sheet surface melt if the observed recent circulation anomalies persist over subsequent decades. Major uncertainties concerning the global understanding of the processes producing these blocking events currently preclude reliable simulation of their occurrence by climate models (Woollings et al., 2018; Smith et al., 2020). Therefore, future ESM developments should focus on representing such changes in atmospheric circulation in order to reduce the uncertainty in: (1) projections of Greenland ice sheet contribution to global sea level rise; and (2) possible downstream effects of Greenland blocking on the North Atlantic polar jet stream and accompanying extreme weather conditions over Northwest Europe (Hanna et al., 2018b).

### **Acknowledgements**

We acknowledge the World Climate Research Programme's (WCRP) Working Group on Coupled Modelling, which is responsible for CMIP, and we thank the climate modelling groups for producing and making available their model output. EH acknowledges support from WCRP CliC that helped to facilitate discussion. For CMIP the U.S. Department of Energy's Program for Climate Model Diagnosis and Intercomparison provides coordinating support and led development of software infrastructure in partnership with the Global Organization for Earth System Science Portals. NCEP-NCAR-v1 reanalysis are provided by the NOAA/OAR/ESRL PSD, Boulder, Colorado, USA, from their Web site at <https://www.esrl.noaa.gov/psd/>. ERA5 reanalysis are provided by Copernicus Climate Change Service Information (2020) from their website at <https://cds.climate.copernicus.eu>. Alison Delhasse is Research Fellow from the Fonds de la Recherche Scientifique de Belgique (F.R.S.-FNRS).

### **Conflict of interest**

The authors declare that they have no conflict of interest.

### **References**

Andrews, T., Andrews, M. B., Bodas-Salcedo, A., Jones, G. S., Kulmbrodt, T., Manners, J., Menary, M. B., Ridley, J., Ringer, M. A., Sellar, A. A., Senior, C. A. and Tang, Y. (2019) Forcings, feedbacks

and climate sensitivity in HadGEM3-GC3.1 and UKESM1. Submitted to Journal of Advances in Modeling Earth Systems, 0–3. DOI: 10.1029/2019MS001866.

Belleflamme, A., Fettweis, X. and Erpicum, M. (2015) Recent summer Arctic atmospheric circulation anomalies in a historical perspective. *Cryosphere*, 9, 53–64. DOI: 10.5194/tc-9-53-2015.

Delhasse, A., Fettweis, X., Kittel, C., Amory, C. and Agosta, C. (2018) Brief communication: Impact of the recent atmospheric circulation change in summer on the future surface mass balance of the Greenland ice sheet. *The Cryosphere*, 12, 3409–3418. DOI: 10.5194/tc-2018-65.

Eyring, V., Bony, S., Meehl, G. A., Senior, C. A., Stevens, B., Stouffer, R. J. and Taylor, K. E. (2016) Overview of the Coupled Model Intercomparison Project Phase 6 (CMIP6) experimental design and organization. *Geoscientific Model Development*, 9, 1937–1958. DOI: 10.5194/gmd-9-1937-2016.

Fang, Z.-F. (2004) Statistical relationship between the northern hemisphere sea ice and atmospheric circulation during winter time. 131–141.

Fettweis, X., Franco, B., Tedesco, M., van Angelen, J. H., Lenaerts, J. T. M., van den Broeke, M. R. and Gallée, H. (2013a) Estimating Greenland ice sheet surface mass balance contribution to future sea level rise using the regional atmospheric climate model MAR. *The Cryosphere*, 7, 469–489. DOI: 10.5194/tcd-6-3101-2012.

Fettweis, X., Hanna, E., Lang, C., Belleflamme, A., Erpicum, M. and Gallée, H. (2013b) Brief communication Important role of the mid-tropospheric atmospheric circulation in the recent surface melt increase over the Greenland ice sheet. *Cryosphere*, 7, 241–248. DOI: 10.5194/tc-7-241-2013.

Fettweis, X., Box, J. E., Agosta, C., Amory, C., Kittel, C. and Gallée, H. (2017) Reconstructions of the 1900–2015 Greenland ice sheet surface mass balance using the regional climate MAR model. *The Cryosphere*, 1015–1033. DOI: 10.5194/tc-11-1015-2017.

Gettelman, A., Hannay, C., Bacmeister, J. T., Neale, R. B., Pendergrass, A. G., Danabasoglu, G., Lamarque, J., Fasullo, J. T., Bailey, D. A., Lawrence, D. M. and Mills, M. J. (2019) High Climate Sensitivity in the Community Earth System Model Version 2 (CESM2). *Geophysical Research Letters*, 46, 8329–8337. DOI: 10.1029/2019gl083978.

Gidden, M. J., Riahi, K., Smith, S. J., Fujimori, S., Luderer, G., Kriegler, E., Vuuren, D. P. V., Berg, M. V. D., Feng, L., Klein, D., Calvin, K., Doelman, C., Frank, S., Fricko, O., Harmsen, M., Hasegawa, T., Havlik, P., Hilaire, J., Hoesly, R., Horing, J., Popp, A., Stehfest, E. and Takahashi, K. (2019) Global emissions pathways under different socioeconomic scenarios for use in CMIP6 : a dataset of harmonized emissions trajectories through the end of the century. *Geoscientific Model Development*, 12, 1443–1475. DOI: 10.5194/gmd-12-1443-2019.

Hanna, E., Jones, J. M., Cappelen, J., Mernild, S. H., Wood, L., Steffen, K. and Huybrechts, P. (2013) The influence of North Atlantic atmospheric and oceanic forcing effects on 1900–2010 Greenland summer climate and ice melt/runoff. *International Journal of Climatology*, 33, 862–880. DOI: 10.1002/joc.3475.

Hanna, E., Fettweis, X., Mernild, S. H., Cappelen, J., Ribergaard, M. H., Shuman, C. A., Steffen, K., Wood, L. and Mote, T. L. (2014) Atmospheric and oceanic climate forcing of the exceptional Greenland ice sheet surface melt in summer 2012. *International Journal of Climatology*, 34, 1022–1037. DOI: 10.1002/joc.3743.

Hanna, E., Cropper, T. E., Jones, P. D., Scaife, A. A. and Allan, R. (2015) Recent seasonal asymmetric changes in the NAO (a marked summer decline and increased winter variability) and associated changes in the AO and Greenland Blocking Index. *International Journal of Climatology*, 35, 2540–2554. DOI: 10.1002/joc.4157.

Hanna, E., Cropper, T. E., Hall, R. J. and Cappelen, J. (2016) Greenland Blocking Index 1851–2015: a regional climate change signal. *International Journal of Climatology*, 36, 4847–4861. DOI: 10.1002/joc.4673.

Hanna, E., Fettweis, X. and Hall, R. J. (2018a) Recent changes in summer Greenland blocking captured by none of the CMIP5 models. *The Cryosphere*, 3287–3292. DOI: 10.5194/tc-12-3287-2018.

Hanna, E., Hall, R. J., Cropper, T. E., Ballinger, T. J., Wake, L., Mote, T. and Cappelen, J. (2018b) Greenland blocking index daily series 1851–2015: Analysis of changes in extremes and links with North Atlantic and UK climate variability and change. *International Journal of Climatology*, 38, 3546–3564. DOI: 10.1002/joc.5516.

Hanna, E., Cappelen, J., Fettweis, X., Mernild, S. H., Mote, T. L., Mottram, R., Steffen, K., Ballinger, T. J. and Hall, R. (2020) Greenland surface air temperature changes from 1981 to 2019 and implications for ice-sheet melt and mass-balance change. *International Journal of Climatology*. DOI: 10.1002/joc.6771.

Hersbach, H., Bell, B., Berrisford, P., Hirahara, S., Horányi, A., Muñoz-Sabater, J., Nicolas, J., Peubey, C., Radu, R., Schepers, D., Simmons, A., Soci, C., Abdalla, S., Abellan, X., Balsamo, G., Bechtold, P., Biavati, G., Bidlot, J., Bonavita, M., Chiara, G., Dahlgren, P., Dee, D., Diamantakis, M., Dragani, R., Flemming, J., Forbes, R., Fuentes, M., Geer, A., Haimberger, L., Healy, S., Hogan, R. J., Hólm, E., Janisková, M., Keeley, S., Laloyaux, P., Lopez, P., Lupu, C., Radnoti, G., Rosnay, P., Rozum, I., Vamborg, F., Villaume, S. and Thépaut, J. (2020) The ERA5 Global Reanalysis. *Quarterly Journal of the Royal Meteorological Society*. DOI: 10.1002/qj.3803.

Hofer, S., Tedstone, A. J., Fettweis, X. and Bamber, J. L. (2017) Decreasing cloud cover drives the recent mass loss on the Greenland Ice Sheet. *Science Advances*, 3, e1700584. DOI: 10.1126/sciadv.1700584.

Hofer, S., Lang, C., Amory, C., Kittel, C., Delhasse, A., Tedstone, A. and Fettweis, X. (2020) Greater Greenland Ice Sheet contribution to global sea level rise in CMIP6. *Nature Communications*, 11, 6289. DOI: 10.1038/s41467-020-20011-8

Kalnay, E., Kanamitsu, M., Kistler, R., Collins, W., Deaven, D., Gandin, L., Iredell, M., Saha, S., White, G., Woollen, J., Zhu, Y., Chelliah, M., Ebisuzaki, W., Higgins, W., Janowiak, J., Mo, K. C., Ropelewski, C., Wang, J., Leetmaa, A., Reynolds, R., Jenne, R. and Joseph, D. (1996) The ncep/ncar 40-year reanalysis project. *Bulletin of the American Meteorological Society*, 77, 437–472. DOI: 10.1175/1520-0477(1996)077<0437:TNYRP>2.0.CO;2.

McLeod, J. T. and Mote, T. L. (2016) Linking interannual variability in extreme Greenland blocking episodes to the recent increase in summer melting across the Greenland ice sheet. *International Journal of Climatology*, 36, 1484–1499. DOI: 10.1002/joc.4440.

Noël, B., van de Berg, W. J., Lhermitte, S. and van den Broeke, M. R. (2019) Rapid ablation zone expansion amplifies north Greenland mass loss. *Science Advances*, 5, 2–11. DOI:10.1126/sciadv.aaw0123.

O'Neill, B. C., Tebaldi, C., Van Vuuren, D. P., Eyring, V., Friedlingstein, P., Hurtt, G., Knutti, R., Kriegler, E., Lamarque, J. F., Lowe, J., Meehl, G. A., Moss, R., Riahi, K. and Sanderson, B. M. (2016) The Scenario Model Intercomparison Project (ScenarioMIP) for CMIP6. *Geoscientific Model Development*, 9, 3461–3482. DOI: 10.5194/gmd-9-3461-2016.

Overland, J. E., Francis, J. A., Hanna, E. and Wang, M. (2012) The recent shift in early summer Arctic atmospheric circulation. *Geophysical Research Letters*, 39, 1–6. DOI:10.1029/2012GL053268.

Smith, D. M., Scaife, A. A., Eade, R., Athanasiadis, P., Bellucci, A., Bethke, I., Bilbao, R., Borchert, L. F., Caron, L. P., Counillon, F., Danabasoglu, G., Delworth, T., Doblas-Reyes, F. J., Dunstone, N. J., Estella-Perez, V., Flavoni, S., Hermanson, L., Keenlyside, N., Kharin, V., Kimoto, M., Merryfield, W. J., Mignot, J., Mochizuki, T., Modali, K., Monerie, P. A., Müller, W. A., Nicolí, D., Ortega, P., Pankatz, K., Pohlmann, H., Robson, J., Ruggieri, P., Sospedra-Alfonso, R., Swingedouw, D., Wang, Y., Wild, S., Yeager, S., Yang, X., Zhang, L. (2020). North Atlantic climate far more predictable than models imply. *Nature*, 583(7818), 796–800. <https://doi.org/10.1038/s41586-020-2525-0>

Taylor, K. E., Stouffer, R. J. and Meehl, G. A. (2012) An overview of CMIP5 and the experiment design. *Bulletin of the American Meteorological Society*, 93, 485–498. DOI: 10.1175/BAMS-D-11-00094.1.

Tedesco, M., Fettweis, X., Mote, T., Wahr, J., Alexander, P., Box, J. E. and Wouters, B. (2013) Evidence and analysis of 2012 Greenland records from spaceborne observations, a regional climate model and reanalysis data. *The Cryosphere*, 7, 615–630. DOI: 10.5194/tc-7-615-2013.

Tedesco, M., Mote, T., Fettweis, X., Hanna, E., Jeyaratnam, J., Booth, J. F., Datta, R. and Briggs, K. (2016) Arctic cut-off high drives the poleward shift of a new Greenland melting record. *Nature Communications*, 7, 3–8. DOI:10.1038/ncomms11723.

Tedesco, M. and Fettweis, X. (2020) Unprecedented atmospheric conditions (1948–2019) drive the 2019 exceptional melting season over the Greenland ice sheet. *Cryosphere*, 14, 1209–1223. DOI: 10.5194/tc-14-1209-2020.

Trusel, L. D., Das, S. B., Osman, M. B., Evans, M. J., Smith, B. E., Fettweis, X., McConnell, J. R., Noël, B. P. Y. and van den Broeke, M. R. (2018) Nonlinear rise in Greenland runoff in response to post-industrial Arctic warming. *Nature*, 564, 104–108. DOI:10.1038/s41586-018-0752-4.

van den Broeke, M. R., Enderlin, E. M., Howat, I. M., Kuipers Munneke, P., Noël, B. P., Jan Van De Berg, W., Van Meijgaard, E. and Wouters, B. (2016) On the recent contribution of the Greenland ice sheet to sea level change. *The Cryosphere*, 10, 1933–1946. DOI: 10.5194/tc-10-1933-2016.

Voldoire, A., Saint-Martin, D., Sénési, S., Decharme, B., Alias, A., Chevallier, M., Colin, J., Guérémy, J. F., Michou, M., Moine, M. P., Nabat, P., Roehrig, R., Salas y Méliá, D., Séférián, R., Valcke, S., Beau, I., Belamari, S., Berthet, S., Cassou, C., Cattiaux, J., Deshayes, J., Douville, H., Ethé, C., Franchistéguy, L., Geoffroy, O., Lévy, C., Madec, G., Meurdesoif, Y., Msadek, R., Ribes, A., Sanchez-Gomez, E., Terray, L. and Waldman, R. (2019) Evaluation of CMIP6 DECK



Experiments With CNRM-CM6-1. *Journal of Advances in Modeling Earth Systems*, 11, 2177–2213. DOI: 10.1029/2019MS001683.

Woollings, T., Barriopedro, D., Methven, J., Son, S. W., Martius, O., Harvey, B., Sillmann, J., Lupo, A. R. and Seneviratne, S. (2018) Blocking and its Response to Climate Change. *Current Climate Change Reports*, 4, 287–300. DOI: 10.1007/s40641-018-0108-z.

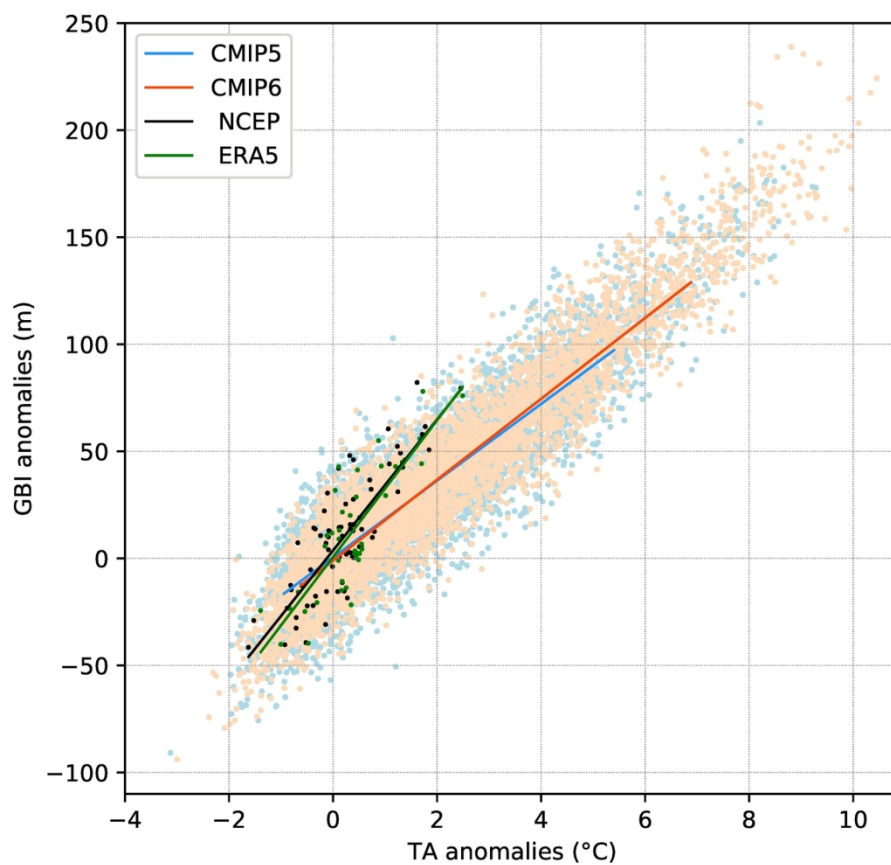


Figure 1. Scatter plot of Greenland Blocking Index (GBI) anomalies vs mean free temperature anomalies (TA) defined as the mean 850, 700 and 500 hPa temperature anomalies (TA) over 60–80 °N, 20–80 °W. The reference period is 1980 – 1999.

GBI correlation with TA				
	$r^2$	(1948-2019)	(2019-2100)	(1948-2100)
<b>CMIP5</b>	P05	0.53	0.73	0.82
	P95	0.71	0.86	0.91
	Mean	0.51	0.73	0.81
<b>CMIP6</b>	P05	0.62	0.85	0.89
	P95	0.77	0.92	0.94
	Mean	0.61	0.81	0.87
<b>NCEP</b>	(1950-2019)	0.68		
<b>ERA5</b>	(1979-2019)	0.70		

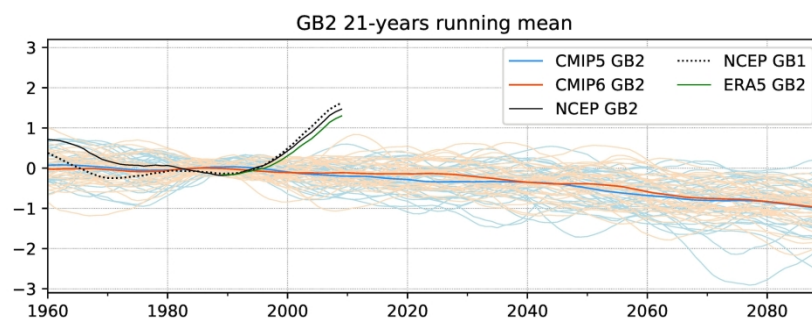


Figure 2. JJA GB1 (dashed black line) and GB2 (solid black line, defined in Eq. 2) indices over 1950 – 2100 as simulated by NCEP/NCAR Reanalysis 1, ERA5 Reanalysis (green line), as well as by all the CMIP5 models (RCP8.5 scenario, blue lines) and the CMIP6 models (ssp585, red lines). Lighter lines represent the normalized GB2 for each model while the mean of CMIP5 and CMIP6 models are represented by the thicker lines. The historical scenario is used from 1950 – 2005 for CMIP5 and 1950 – 2014 for CMIP6, while RCP8.5 and ssp585 are respectively used afterwards. Finally a 21-year running mean has been used to smooth the time series, and values have been normalized using 1980 – 1999 as the reference period.



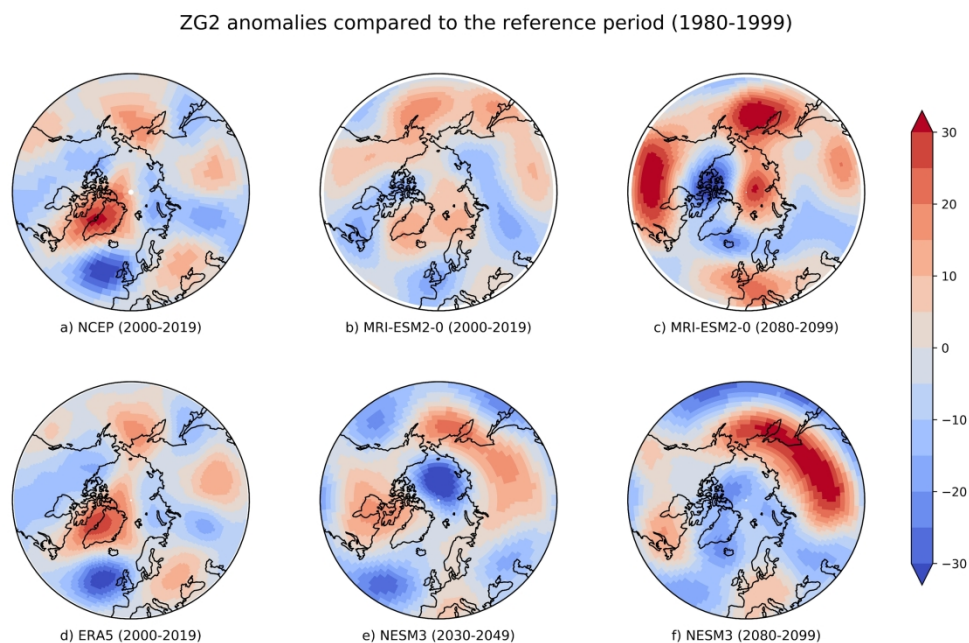
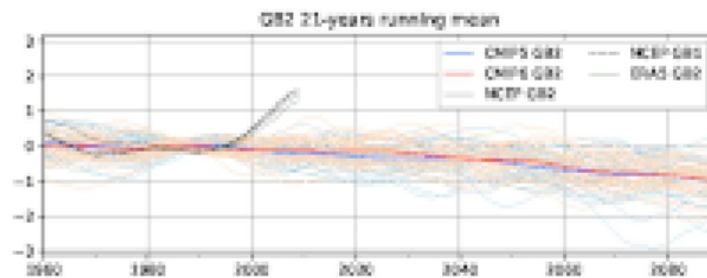


Figure 3. ZG2 anomalies (m) over 2000 – 2019 for a) NCEP, b) ERA5 reanalysis with respect to the reference period (1980 – 1999). Similar for MRI-ESM2-0 over 2000 – 2019 (b), 2080 – 2099 (c) and NESM3 over 2030 – 2049 (e) and 2080 – 2099 (f). ZG2 was computed by removing the mean Z500 between 60 °N and 80 °N to remove the artificial increase in geopotential height due to global warming.



The GBI index is used to assess the occurrence of blocking events in Greenland that have become increasingly prevalent over the last 20 years. It is used here to evaluate the representation of such events up to 2100 by the new generation of CMIP6 ESMs in comparison with the previous generation (CMIP5) and climate reanalyses. Impacting by various feedbacks the surface melt of the ice sheet, the non-representation of these events by CMIP6 models could result in future melt increases being underestimated if such a pattern of atmospheric circulation persists in the coming decades.